Contribution from Chemistry Department A, Building 207, The Technical University of Denmark, DK-2800 Lyngby, Denmark, and Department of Chemistry, The University of Aarhus, Langelandsgade 140, DK-8000 Aarhus C, Denmark

Direct and Superexchange Electron Tunneling at the Adjacent and Remote Sites of Higher Plant Plastocyanins

Hans E. M. Christensen,[†] Lars S. Conrad,[†] Kurt V. Mikkelsen,[‡] Martin K. Nielsen,[†] and Jens Ulstrup*[,†]

Received October 30, 1989

The 42-45 and 59-61 residues of several higher plant plastocyanins are ionized at neutral pH. The resulting negative charges constitute a binding site for positively charged electron-transfer (ET) reactants even though the ET distances exceed the distance at the adjacent binding site close to the solvent-exposed His-87 ligand by 5-10 Å. We have calculated the exchange matrix elements, V_{DA}, for ET between plastocyanin and the protonated pyridine anion radical as a probe for small reaction partners by superexchange and extended Hückel theory. Adjacent binding-site ET and four ET routes along different amino acid sequences from the copper atom toward the remote binding site through the protein are compared. One route, Cu/Met-92/Phe-14/Phe-82, is very inefficient ($V_{DA} = 1 \times 10^{-9}$ cm^{-1}) due to its through-space character and perpendicular phenyl group orientation. ET along two other routes, Cu/Met-92/Val-93/Gly-94 ($V_{DA} = 3 \times 10^{-4}$ cm^{-1}) and Cu/Cys-84/Tyr-83/Phe-82 ($V_{DA} = 6 \times 10^{-4}$ cm^{-1}), is much more facile, but only the Cu/Cys-84/Tyr-83 route ($V_{DA} = 6 \times 10^{-2}$ cm^{-1}) approaches the adjacent site efficiency ($V_{DA} = 0.4$ cm^{-1}), in line with many observations of a crucial role for Tyr-83. The results suggest that ET through the protein is dominated by selective through-bond pathways rather than simple geometric distance correlations and that remote site reactivity may rest on both favorable work terms and competitive electronic factors.

1. Introduction

The detailed electron-transfer (ET) route between suitable surface sites on redox metalloproteins and their metal centers is of considerable current interest.[1-10] This relates to the fundamental physical mechanism of protein ET, to ET in organized photosynthetic[11,12] and respiratory[13] membrane systems, and to potential protein function in molecular devices.[14] Many reports have documented that "long-range" ET can be brought to occur in metalloprotein systems modified by the attachment of electron-exchanging surface groups.[1-8] These investigations have pointed to the crucial importance of interreactant group distance and orientation, to the nature of the intermediate protein matter, and to both nuclear and electronic effects caused by configurational dynamics, i.e. to nonequilibrium features of the collective protein modes at the moment of electron transfer.

Both data for small metalloprotein ET[1-9,15-21] and expectation from ET theory[21-25] show that attention to the "natural" electron percolation routes of unmodified metalloproteins with asymmetrically located metal atoms inside the protein is also important. ET patterns of such proteins might for example illuminate whether proteins always exploit the shortest ET route or whether either surface structural elements or molecular and electronic properties of the protein provide other, longer range but more facile ET routes. The ET patterns of the photosynthetic blue single-copper protein plastocyanin (PC), broadly investigated in many reports in recent years,[8,16] constitute a suitable case for further examination of this important question. Many strong indications suggest that this protein in fact exploits two major different routes with widely different ET distances and surface structural features. In this work we briefly discuss data from several recent reports that substantiate this view, and we offer a simple theoretical frame based on superexchange theory and extended Hückel calculations and on local surface charge effects to account for the comparable ET rates along the two routes.

2. Electron Transfer at the Adjacent and Remote Binding Sites of Higher Plant Plastocyanins

Many recent investigations provide strong support for the view that higher plant PC can indeed exploit two molecular ET pathways.[4,8,15-21,26-30] One pathway involves electron exchange at the electrically neutral hydrophobic surface site (the adjacent or "north" site) close to the strongly asymmetrically located copper atom, the His-87 ligand of which is exposed to the external solvent. The other path is based on electron exchange at the remote (or "east") site, substantially farther (≈15 Å) from the copper atom. In PC from spinach, poplar, and other higher plants this site is dominated by a conserved, highly negatively charged area constituted by the carboxylate groups in the 42-45 and 59-61 residues,

[†] The Technical University of Denmark.
[‡] The University of Aarhus.

(1) Nocera, D. G.; Winkler, J. R.; Yocom, K. M.; Bordignon, E.; Gray, H. B. *J. Am. Chem. Soc.* **1984**, *106*, 5145.
(2) Axup, A. W.; Albin, M.; Mayo, S. L.; Crutchley, R. J.; Gray, H. B. *J. Am. Chem. Soc.* **1988**, *110*, 435.
(3) Many contributions in: *Proceedings of the 4th International Conference on Bioinorganic Chemistry. J. Inorg. Biochem.* **1989**, *36*, 151-372.
(4) Jackman, M. P.; Sykes, A. G.; Salmon, A. G. *J. Chem. Soc., Chem. Commun.* **1987**, 65.
(5) Jackman, M. P.; Lim, M.-C.; Sykes, A. G.; Salmon, G. A. *J. Chem. Soc., Dalton Trans.* **1988**, 2843.
(6) Jackman, M. P.; McGinnis, J.; Powls, R.; Salmon, G. A.; Sykes, A. G. *J. Am. Chem. Soc.* **1988**, 5880.
(7) Isied, S. S.; Kuehn, C.; Worosila, G. *J. Am. Chem. Soc.* **1984**, *106*, 1722.
(8) Farver, O.; Pecht, I. *Coord. Chem. Rev.* **1989**, *94*, 17.
(9) McLendon, G. *Acc. Chem. Res.* **1988**, *21*, 160.
(10) Mikkelsen, K. V.; Ulstrup, J.; Zakaraya, M. G. *J. Am. Chem. Soc.* **1989**, *111*, 1315.
(11) *The Photosynthetic Bacterial Reaction Center. Structure and Dynamics*; Breton, J., Vermêglio, A., Eds.; Plenum: New York, 1988.
(12) *Perspectives in Photosynthesis*; Jortner, J., Pullman, A., Eds.; Kluwer: Dordrecht, The Netherlands, 1990.
(13) DeVault, D. *Quantum Mechanical Tunnelling in Biological Systems*; Cambridge University Press: Cambridge, England, 1984.
(14) *Molecular Electronic Devices*; Carter, F. L., Siatkowski, R. E., Wohltjen, H., Eds.; North-Holland: Amsterdam, 1988.
(15) (a) Williams, G.; Moore, G. R.; Williams, R. P. J. *Comments Inorg. Chem.* **1985**, *4*, 55. (b) Cusanovich, M. A.; Meyer, T. E.; Tollin, G. In *Heme Proteins*; Eicchorn, G. L., Marzilli, L. G., Eds.; Elsevier: Amsterdam, 1988; Vol. VII, p 37.
(16) Sykes, A. G. *Chem. Soc. Rev.* **1985**, *14*, 283.
(17) (a) Segal, M. G.; Sykes, A. G.; *J. Am. Chem. Soc.* **1978**, *100*, 4585. (b) Jackman, M. P.; McGinnis, J.; Sykes, A. G.; Collyer, C. A.; Murata, M.; Freeman, H. C. *J. Chem. Soc., Dalton Trans.* **1987**, 2573.
(18) Sinclair-Day, J. D.; Sykes, A. G. *J. Chem. Soc., Dalton Trans.* **1986**, 2069.
(19) McGinnis, J.; Sinclair, J. D.; Sykes, A. G. *J. Chem. Soc., Dalton Trans.* **1986**, 2007.
(20) Pladziewicz, J. R.; Brenner, M. S. *Inorg. Chem.* **1987**, *26*, 3629.
(21) Christensen, H. E. M.; Ulstrup, J.; Sykes, A. G. *Biochim. Biophys. Acta*, in press.
(22) (a) Dogonadze, R. R.; Kuznetsov, A. M. *Physical Chemistry. Kinetics*; VINITI: Moscow, 1973. (b) Dogonadze, R. R.; Kuznetsov, A. M. *Prog. Surf. Sci.* **1975**, *6*, 1. (c) Dogonadze, R. R.; Kuznetsov, A. M. *Kinetics and Catalysis*; VINITI: Moscow, 1978.
(23) Ulstrup, J. *Charge Transfer Processes in Condensed Media*; Springer-Verlag: Berlin, 1979.
(24) Kuznetsov, A. M. *Electrochim. Acta* **1987**, *32*, 1271.
(25) Kuznetsov, A. M.; Ulstrup, J.; Vorotyntsev, M. A. In *The Chemical Physics of Solvation. Part C. Solvation in Specific Physical, Chemical and Biological Systems*; Dogonadze, R. R., Kálmán, E., Kornyshev, A. A., Ulstrup, J., Eds.; Elsevier: Amsterdam, 1988; p 163.
(26) Lappin, A. G.; Segal, M. G.; Weatherburn, D. G.; Sykes, A. G. *J. Am. Chem. Soc.* **1979**, *101*, 2297.
(27) (a) Cookson, D. J.; Hayes, M. T.; Wright, P. E. *Nature* **1980**, *283*, 682. (b) Cookson, D. J.; Hayes, M. T.; Wright, P. E. *Biochim. Biophys. Acta* **1980**, *591*, 162.

0020-1669/90/1329-2808$02.50/0

which undoubtedly helps to make this longer range ET path more facile for positively charged reaction partners. The negatively charged area is not conserved for blue-green bacterial PC's, for which, interestingly, remote-site ET is not explicitly documented either.[31,32]

The documentation for dual-path ET in higher plant PC can be summarized in the following points:

(a) Two frequently applied ionic redox couples in small protein investigations are $[Fe(CN)_6]^{3-/4-}$ and $[Co(phen)_3]^{3+/2+}$ (phen = 1,10-phenanthroline).[16-19,21] NMR and blocking experiments point to binding of the structurally analogous but redox-inactive ions $[Cr(CN)_6]^{3+}$ and $[Cr(phen)_3]^{3+}$ solely at the adjacent (close to His-87) and remote site (close to Tyr-83), respectively.[26-29] This suggests that both areas constitute electron-exchange sites and that ionic charge is important in selection of the preferred ET route.

(b) Attachment of $[Cr(H_2O)_6]^{2+}$ to PC(II), thermolysin degradation subsequent to intramolecular ET, and isolation of the peptide fragments show that the resulting Cr(III) is bound preferentially to the 42–45 residues.[8,33] This suggests that the remote site has been the locus for electron transfer.

(c) $[Co(phen)_3]^{3+}$ and other strongly positively charged ions exhibit saturation kinetics, indicative of strong binding.[16,19] This is likely to be at the negatively charged site. No saturation kinetics is encountered for negatively charged ions or for blue-green bacterial PC.[31,32]

(d) Strongly positively charged redox-inactive ions induce inhibition.[20,34] This is usually interpreted as blocking of the remote site and allows separation of the kinetics into adjacent- and remote-site contributions. The fact that weakly positively charged ions (ferrocenium ions[20]) still react comparably at both sites suggests, however, that also electronic effects determine the reactivity along the two paths.

(e) The rate constants for ET between PC and positively charged ions at neutral pH decrease with increasing ionic strength,[35,36] indicative of a negatively charged surface site. The ionic strength dependence is weaker at lower pH where the remote site is blocked.[36]

(f) The pH profiles of the rate constants for oxidation of spinach PC(I) by $[Fe(CN)_6]^{3-}$ and $[Co(phen)_3]^{3+}$ are notably different.[16-19,21] The former avoids the remote site and gives pK values that coincide with values determined by NMR spectroscopy and represents protonation of coordinated His-87. The pH profile for $[Co(phen)_3]^{3+}$ is a composite of two protonations, one of which involves His-87. The other one corresponds to a higher pK and represents protonation most likely at the remote site. His-87 of PC(II) is not protonated. The pH profile for reduction with positively charged reactants still corresponds to a single protonation, most likely at the remote site, and points to a significant role for this site also in PC(II) reduction.[16-19]

All the effects listed in points B and C–F also relate to the natural reaction partner of PC, cyt f.[37,38] Two other points are as follows:

(g) Kinetic data for the quenching of excited states of $[CrL_3]^{3+}$ and $[RuL_3]^{2+}$ (L = phen, 2,2'-bipyridine) by ET from PC(I) suggest that both sites contribute to the overall kinetics.[30]

(h) Nitro modification of PC Tyr-83 leads to both a 20-mV redox potential increase and lowering of the Tyr-83 pK of at least 2 units.[21] A new branch also appears in the pH profiles of both the redox potential and the ET rate constant. The redox potential and work term changes induced by nitro modification are reflected in the rate constants for ET between PC and both the $[Fe(CN)_6]^{3-/4-}$ and $[Co(phen)_3]^{3+/2+}$ couples, and the correlations are well in line with ET theory,[22-25,39-41] substantiating ET close to Tyr.[21]

The pattern summarized above is broadly representative of PC from spinach, French bean, parsley, and poplar, even though some variation in residue composition at the binding site and kinetic detail is encountered. The data are strongly indicative of both an ET path along the remote site channel and "direct" ET at the exposed His-87. The data also suggest that local surface charges are crucial in providing documentation for the ET path and in endowing the long-range channel with appropriate efficiency.

Surface charges and favorable ET work terms are, however, not necessarily the only reason why the remote site channel is competitive. The following data suggest that this channel is also electronically competitive:

(1) Spinach PC oxidation with weakly charged hydrophobic ferrocenium ions also occurs comparably at both sites,[20] although with more favorable adjacent/remote-distribution ratios.

(2) PC(I) from the blue-green bacterium *Anabaena variabilis* has an overall positive charge of 1+ rather than 9– as for spinach PC(I) and no charge accumulation at the remote site.[31] In line with this the kinetics of PC(I) oxidation by $[Co(phen)_3]^{3+}$ exhibits neither saturation kinetics, inhibition, nor $[Cr(phen)_3]^{3+}$-induced Tyr-83 line broadening,[32] and the rate constant is lower than that for spinach PC by a factor of 5. The ET process is, however, inhibited by remote-site protonation.[32] Dual-path ET could thus prevail also for this PC.

(3) Recent investigations of PC(I) oxidation by $[Co(phen)_3]^{3+}$ and the structurally analogous but electrically neutral substituted complex $[Co(phen\text{-}SO_3)_3]$, i.e.[36]

$$PC(I) + [Co(phen)_3]^{3+} \rightarrow PC(II) + [Co(phen)_3]^{2+} \quad (1)$$

$$PC(I) + [Co(phen\text{-}SO_3)_3] \rightarrow PC(II) + [Co(phen\text{-}SO_3)_3]^{-} \quad (2)$$

have provided a separation of the adjacent/remote-distribution ratio into a work term component and an electronic component.[36] The choice of this probe system was promoted by the following consideration:

(a) The two Co(II) complexes have almost the same structure and reorganization parameters.

(b) Their different charges provide a precise clue to the work terms for $[Co(phen)_3]^{3+}$.

(c) Their ET pattern toward small reactants is well represented in detail by the simplest models of ET theory such as hard conducting spheres and structureless dielectric media.[42] They can therefore be expected to be useful "probes" for molecular interactions on a protein surface, as indicated by a previous report on the reactions of the two Co(III) complexes with cyt c.[43]

Details of the experimental investigations for the reactions in eqs 1 and 2 will be given elsewhere.[36] Presently, we notice that ET features based on pH and ionic strength variation of the rate constants combined with ET theory have indicated that the rate constant ratio at the adjacent and remote sites amount to about 7:3 for the neutral and 1:7 for the positively charged complex. These values suggest that also neutral complexes can react comparably at both sites. Effects other than work terms therefore contribute to favorable long-range ET through the protein. In

(28) Handford, P. M.; Hill, H. A. O.; Lee, W.-K.; Henderson, R. A.; Sykes, A. G. *J. Inorg. Biochem.* **1980**, *13*, 83.
(29) Armstrong, F. A.; Driscoll, P. C.; Hill, H. A. O.; Redfield, C. *Biochem. Soc. Trans.* **1987**, *15*, 767.
(30) Brunschwig, B. S.; DelAive, P. J.; English, A. M.; Goldberg, M.; Gray, H. B.; Mayo, S. L.; Sutin, N. *Inorg. Chem.* **1985**, *24*, 3743.
(31) Armstrong, G. D.; Chapman, S. K.; Sisley, M. J.; Sykes, A. G.; Aitken, A.; Osherhoff, N.; Margolisah, E. *Biochemistry* **1986**, *25*, 6947.
(32) Jackman, M. P.; Sinclair-Day, J. D.; Sisley, M. J.; Sykes, A. G.; Denys, L. A.; Wright, P. E. *J. Am. Chem. Soc.* **1987**, *109*, 6443.
(33) Farver, O.; Pecht, I. *Proc. Natl. Acad. Sci. U.S.A.* **1981**, *78*, 4190.
(34) Chapman, S. K.; Watson, A. D.; Sykes, A. G. *J. Chem. Soc., Dalton Trans.* **1983**, 2543.
(35) McArdle, J. V.; Coyle, C. L.; Gray, H. B.; Yoneda, G. S.; Holwerda, R. A. *J. Am. Chem. Soc.* **1977**, *99*, 2483.
(36) Christensen, H. E. M.; Conrad, L. S.; Nielsen, M. K.; Ulstrup, J. Manuscript in preparation.
(37) (a) Beoku-Betts, D.; Sykes, A. G. *Inorg. Chem.* **1985**, *24*, 1142. (b) Beoku-Betts, D.; Chapman, S. K.; Knox, C. V.; Sykes, A. G. *Inorg. Chem.* **1985**, *24*, 1677.
(38) Takabe, T.; Ishikawa, H.; Niwa, S.; Tanaka, Y. *J. Biochem.* **1984**, *96*, 385.
(39) Marcus, R. A. *J. Chem. Phys.* **1956**, *24*, 966.
(40) Newton, M. D.; Sutin, N. *Annu. Rev. Phys. Chem.* **1984**, *35*, 437.
(41) Marcus, R. A.; Sutin, N. *Biochim. Biophys. Acta* **1985**, *811*, 265.
(42) Kjaer, A. M.; Ulstrup, J. *Inorg. Chem.* **1986**, *25*, 644.
(43) Kjaer, A. M.; Ulstrup, J. *Inorg. Chem.* **1987**, *26*, 2052.

the next two sections we shall attend to the most conspicuous of such effects, namely the electronic tunnel factor in the diabatic ET rate constant.

3. Direct and Superexchange Electron Tunneling in Plastocyanin ET

In this section we approach the electronic tunnel factor in the diabatic ET process at the adjacent and remote PC sites in a simple way based on superexchange and higher order perturbation theory. Simple estimates of the electron-exchange matrix elements and energy gaps show that long-range ET channels may be fully competitive with ET at the adjacent binding site. In the following section we substantiate this conclusion by quantum chemical calculations on the extended Hückel level which show that real protein ET channels in PC indeed do lead to favorable long-range ET but also that the different through-bond ET channels are highly selective for electron percolation through the protein.

We introduce the following form of the second-order rate constant, k_r, known from ET theory[22-25,40,44]

$$k_r = \kappa \frac{\omega_{eff}}{2\pi} \Delta V \exp\left\{-\left[w_r + \frac{(E_r + \Delta G_0 + w_p - w_r)^2}{4E_r} \right] / k_B T \right\} \quad (3)$$

where ΔG_0 is the reaction free energy, E_r is the total molecular, protein, and solvent reorganization free energy, w_r and w_p reactants' and products' work terms, κ is the electronic transmission coefficient, ΔV is the reaction zone, and ω_{eff} is the "effective" vibrational frequency, precise prescriptions for which are available,[45] while k_B is Boltzmann's constant and T is the temperature. Equation 3 is valid for classical harmonic molecular motion provided that the protein and solvent polarization response to electric field changes associated with ET is linear.

The work term and redox potential corrected differences between the rate constants along the adjacent and remote routes must be reflected in corresponding differences in E_r and w_r. In respect to the reorganization free energy the simplest ET theory favors the shorter range route.[41,42,45] This conclusion is supported by dielectric models that incorporate dielectric image forces and protein size effects,[46] but presently we focus solely on the electronic transmission coefficients as a frame for dual-path ET.

We represent the transmission coefficient for both routes in the form

$$\kappa = \kappa_0 \exp(-\alpha|\vec{R}|) \quad (4)$$

where $\vec{R}$ is the distance between the ET centers, κ_0 the value of κ at the encounter distance, and α a measure of the decay rate of the donor and acceptor electronic wave functions.

Equation 4 emerges straightaway from one-electron molecular and tunneling descriptions.[47] The exponential form is substantiated by much more elaborate quantum chemical and path integral calculations[48-54] that rest on many-electron basis sets and frequently incorporate "matter" between the ET centers in the form of covalently attached bridge group electron mediators or individual solvent molecules. A variety of ET systems also provide experimental support for the exponential distance dependence in eq 4. These extend to trapped electrons and radicals in frozen polar and apolar glasses,[55,56] intramolecular ET in binuclear transition-metal complexes[57,58] or organic anions,[59,60] and intramolecular ET in modified metalloproteins.[2] Exponential distance dependence is finally exhibited by solid-state electronic conduction,[61] in metal–insulator–metal systems,[62] and at electrochemical electrode–electrolyte interfaces.[63] Equation 4 is thus broadly representative of ET systems, many-electron effects being reflected in electronic properties of donor, acceptor, and intermediate material, and in the parameters κ_0 and α. In particular, when applied to the two ET routes of PC, we must expect that both the values of κ_0 and α in eq 4 and their physical meaning are different for the two routes. We consider in turn "direct" ET at the adjacent binding site and "indirect", superexchange ET through the protein at the remote binding site.

3.1. ET at the Hydrophobic Adjacent Binding Site. Coordinated His-87 is exposed to the solvent and ET at this site envisaged to occur "directly", close to contact distance. The pattern can, however, differ from outer-sphere ET between small molecules both by the nature of the work terms, which contain repulsive image forces[43,46,64] for charged reactants, and by the reorganization free energy, which contains contributions from an infinite manifold of image charges inside and outside the protein.[46]

The electronic density of the donor and acceptor orbitals are likely to follow those of corresponding transition-metal complexes with hydrophobic ligands. Data for the distance variation in outer-sphere ET involving transition-metal complexes are few, but for a range of ET systems involving aromatic organic radicals and nonaqueous solvents α is about 1.2–1.4 Å^{-1}.[39,41,65] These values are significantly smaller than gas-phase values estimated from ab initio calculations,[50,51] giving 2.4 Å^{-1} for electron exchange in the $[Fe(H_2O)_6]^{2+/3+}$ system[50] and at least 4 Å^{-1} for metallocene electron-exchange systems.[51] This is because solvent molecules provide a favorable and orientation-dependent superexchange contribution to the electronic factor when the donor and acceptor centers are separated,[53,65] as in the ET processes in frozen matrices (cf. section 3.2). A solvent superexchange contribution, facilitating electron percolation through a hydrogen-bond network, could also be important for shorter range ET, as at the PC adjacent site, but possibly less so, as water molecules are now excluded to a considerable extent from the region between the reaction centers by the geometric extension of the reactant groups. The orbital exponent for adjacent ET can therefore be expected to be at least 1.2–1.4 Å^{-1} but lower than 2–4 Å^{-1} as for gas-phase transition-metal complexes.

The decay parameter at the adjacent binding site thus reflects exposure of the electronic wave functions to the solvent and environment. An alternative view to the superexchange concept is to regard the exponential decay parameter as arising from electron tunneling into a barrier, the height of which, B, is determined by the mobility edge of the solvent, i.e.

(44) German, E. D. *Rev. Inorg. Chem.* **1983**, *5*, 123.
(45) Dogonadze, R. R.; Urushadze, Z. D. *J. Electroanal. Chem. Interfacial Electrochem.* **1971**, *32*, 235.
(46) Kharkats, Yu. I.; Ulstrup, J. *Chem. Phys.* **1990**, *141*, 117.
(47) Duke, C. B. In *Tunnelling in Biological Systems*; Chance, B., DeVault, D. C., Frauenfelder, H., Marcus, R. A., Schrieffer, J. C., Sutin, N., Eds.; Academic Press: New York, 1979; p 31.
(48) (a) Larsson, S. *J. Phys. Chem.* **1984**, *88*, 1321. (b) Larsson, S. *Chem. Scr.* **1988**, *28A*, 15.
(49) Beratan, D. N.; Hopfield, J. J. *J. Am. Chem. Soc.* **1984**, *106*, 1584.
(50) Newton, M. D. *Int. J. Quant. Chem. Symp.* **1980**, *14*, 363.
(51) Newton, M. D. In *Perspectives in Photosynthesis*; Jortner, J., Pullman, B., Eds.; Kluwer: Dordrecht, The Netherlands, 1990; p 157.
(52) Mikkelsen, K. V.; Dalgaard, E.; Swanstrøm, P. *J. Phys. Chem.* **1987**, *91*, 3081.
(53) Mikkelsen, K. V.; Ratner, M. A. *Int. J. Quant. Chem. Symp.* **1987**, *21*, 341.
(54) Kuki, A.; Wolynes, P. G. *Science* **1987**, *236*, 1647.
(55) (a) Beitz, J. V.; Miller, J. R. *J. Chem. Phys.* **1979**, *71*, 4579. (b) Miller, J. R.; Beitz, J. V. *J. Chem. Phys.* **1981**, *74*, 6746.
(56) Miller, J. R.; Beitz, J. V. Huddleston, R. K. *J. Am. Chem. Soc.* **1984**, *106*, 5057.
(57) Isied, S. S. *Prog. Inorg. Chem.* **1984**, *32*, 443.
(58) Wasielewski, M. R.; Niemczyk, M. P.; Svec, W. A.; Pewitt, E. B. *J. Am. Chem. Soc.* **1985**, *107*, 1080.
(59) Closs, G. L.; Miller, J. R. *Science* **1988**, *240*, 443.
(60) (a) Hush, N. S. *Coord. Chem. Rev.* **1985**, *64*, 135. (b) Oevering, H.; Paddon-Row, M. N.; Heppener, H.; Oliver, A. M.; Cotsaris, E.; Verhoeven, J. W.; Hush, N. S. *J. Am. Chem. Soc.* **1987**, *109*, 3268.
(61) Böttger, H.; Bryksin, V. V. *Hopping Conduction in Solids*; VCH Publishers: Weinheim, West Germany, 1985.
(62) Duke, C. B. *Tunnelling in Solids*; Academic Press: New York, 1969.
(63) Schmickler, W.; Schultze, J. W. *Mod. Asp. Electrochem.* **1986**, *17*, 357.
(64) Landau, L. D.; Lifshitz, E. M. *Electrodynamics of Continuous Media*; Pergamon: Oxford, England, 1975.
(65) Mikkelsen, K. V.; Ratner, M. A. *Int. J. Quant. Chem. Symp.* **1988**, *22*, 707.
(66) For an overview, see: Mikkelsen, K. V.; Ratner, M. A. *Chem. Rev.* **1987**, *87*, 113.

$$\alpha \approx \frac{1}{\hbar}\sqrt{2m_e B} \tag{5}$$

where m_e is the mass of the electron and $\hbar$ is Planck's constant divided by 2π (cf. ref 67). B is determined by the LUMO of water and, α takes a large value because B and the electronic excitation energy of water are large.

3.2. Superexchange ET at the Remote Binding ("East") Site. The remote-site ET efficiency is understandable if the orbital decay through the protein is smaller than for "direct" or solvent-assisted ET. This requires that the small reaction partner is intimately associated with the protein so that its electronic "tail" is screened from the solvent and modulated primarily by protein in the direction toward the copper center. In a tunnel view this implies that the protein mobility edge is lower than that for water. The corresponding implications of a superexchange or molecular orbital view are that electron exchange integrals and energy gaps between the intermediate amino acid groups and the donor and acceptor groups are more favorable than for direct ET, or ET modulated by solvent superexchange.

Experimental data and ET theory suggest that these conditions may be valid. Data for long-range ET in metalloprotein and related systems are available,[2-9,58,68,69] but precise extraction of individual electronic transmission coefficients is rather model dependent and fraught with ambiguity. On the other hand, variation of the ET distance, by chemical modification at different surface sites of myoglobins and cytochromes, provides distance relations for the intramolecular ET rate constant.[2,3,68] These are fraught with fewer problems in the separation of the electronic factor from the activation entropy, but due to the anisotropy of the protein structure the distance variation represents average correlations over different directions. With this reservation the distance correlation has been found to be approximately exponential for myoglobins, with an orbital decay parameter of 0.9 Å^{-1}.[2] This value is less favorable than those for synthetic ET complexes with corresponding donor–acceptor separation[58,68,69] but lower than those for the solvent-separated ET systems discussed above, which suggests that ET through protein is favored relative to ET subject only to solvent screening. Both tunnel[47,62] and quantum chemical theories[48-53] favor through-bond ET and lower energy bonds over higher energy bonds. This can be visualized straightaway by barrier considerations in tunnel theory.[70,71] In MO and superexchange theory it is reflected in more favorable through-bond exchange matrix elements relative to direct ET, and the more favorable the intermediate-state energy gap denominators, the lower the intermediate-state LUMO's and the more negative the redox potential of the donor group.

We now illustrate this by the following simple formalism that rests on many-electron MO theory but where the MO frame has been reduced to the superexchange limit.[72-74] The transmission coefficient is related to the overall (i.e. direct or superexchange) electron-exchange matrix element by[22,45]

$$\kappa = (T_{DA})^2\sqrt{\frac{4\pi^3}{(\hbar\omega_{eff})^2 E_r k_B T}} \tag{6}$$

in the diabatic limit. The general form of T_{DA} including both

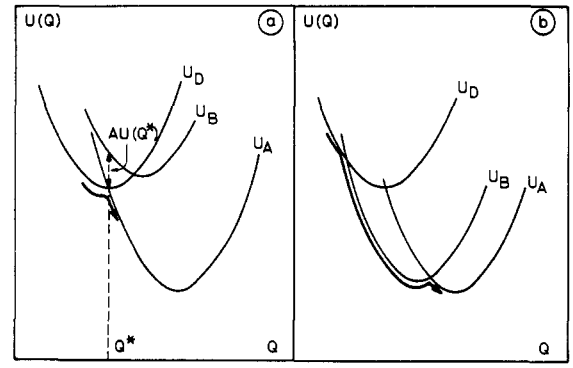

Figure 1. Schematic view of one-dimensional potential energy surfaces for superexchange ET involving a single intermediate state of "high" (a) and "low" (b) energy.

direct and superexchange ET through all conceivable bridge group states, B, emerges from the following separation of the total system Hamiltonian, H, known from scattering theory:[22,75]

$$H = H_D + V_D = H_{B1} + V_{B1} = ... = H_{BN} + V_{BN} = H_A + V_A \tag{7}$$

The subscripts D and A refer to the donor and acceptor channel, respectively, and the B terms, to all the bridge group channels. The H terms are zero-order channel Hamiltonians, and the V terms, perturbations. In principle, $H_D \neq H_{B1} \neq ... H_{BN} \neq H_A$, and the zero-order Hamiltonians are conveniently defined so that they contain the diagonal parts of the perturbation exchange matrix elements, leaving only the nondiagonal parts in the V terms.[22,76]

T_{DA} in eq 5 is obtained by expanding the total scattering operator in an infinite perturbation series.[75] A summary of these steps is given in the Appendix. The first-order terms are $V_{DA}^{(1)} = V_{DA}^{nond}$, where "nond" refers to the nondiagonal part only, i.e.

$$V_{DA}^{nond} = V_{DA} - S_{DA}V_{DD} \tag{8}$$

V_{DD} being the diagonal part of V_D with respect to the donor electronic wave function and S_{DA} the overlap integral. V_{DA}^{nond} represents direct ET from donor to acceptor, unassisted by bridge group orbitals. The second order term is

$$V_{DA}^{(2)} = \sum_{J=1}^{N}\frac{V_{D(BJ)}^{(1)}V_{(BJ)A}^{(1)}}{E_D - E_{BJ}} = \sum_{J=1}^{N}\sum_{\beta}\sum_{m}\frac{V_{D\alpha l,(BJ)\beta m}^{(1)}V_{(BJ)\beta m,A\gamma n}^{(1)}}{E_{D\alpha l} - E_{(BJ)\beta m}} \tag{9}$$

where the nond superscripts have been omitted, while E is the total electronic–vibrational energy of the channel indicated by the subscript. Equation 9 incorporates bridge group assistance by all intermediate groups "J" between the donor and acceptor centers. Each of these groups may contribute by several electronic states, for example by parallel electron and hole transfer. Finally, both the electron-exchange matrix elements and the energy denominators depend on the nuclear configuration at the moment of electron transfer. This feature is incorporated by summation with respect to all electronic (α, β, γ) and vibrational (l, m, n) states in the different bridge groups (reaction channels) in the second part of eq 9. In the following we assume that a particular electronic state on each group dominates and omit the electronic state summation. The Nth order term is then

$$V_{DA}^{(N)} = \frac{V_{D(B1)}^{(1)}V_{(B1)(B2)}^{(1)}...V_{(BN)A}^{(1)}}{(E_D - E_{B1}')(E_D - E_{B2}')...(E_D - E_{BN}')} \tag{10}$$

(67) Bixon, M.; Jortner, J. In *Protein Structure: Molecular and Electronic Reactivity*; Austin, R. H., Bukhs, E., Chance, B., DeVault, D. C., Dutton, P. L., Frauenfelder, H., Gol'danskij, V. I., Eds.; Springer-Verlag: New York, 1987; p 277.
(68) Meade, T. J.; Gray, H. B.; Winkler, J. R. *J. Am. Chem. Soc.* **1989**, *111*, 4353.
(69) Isied, S. S.; Vassilian, A.; Wishart, J. W.; Creutz, C.; Schwarz, H.; Sutin, N. *J. Am. Chem. Soc.* **1988**, *110*, 635.
(70) Ulstrup, J. *Surf. Sci.* **1980**, *101*, 564.
(71) Kuznetsov, A. M.; Ulstrup, J.; Zakaraya, M. G. In *Perspectives in Photosynthesis*; Jortner, J., Pullman, B., Eds.; Kluwer: Dordrecht, The Netherlands, 1990; p 241.
(72) Anderson, P. W. *Phys. Rev.* **1950**, *79*, 350.
(73) Halpern, J.; Orgel, L. E. *Discuss. Faraday Soc.* **1960**, *29*, 32.
(74) McConnell, H. M. *J. Chem. Phys.* **1961**, *35*, 508.
(75) Goldberger, M. L.; Watson, K. M. *Collision Theory*; Wiley: New York, 1964.
(76) Kuznetsov, A. M.; Ulstrup, *J. Faraday Discuss. Chem. Soc.* **1982**, *74*, 31.

where "/" represents correction for exchange splitting between the intermediate states and explicit indication of vibrational state summation has been omitted. The overall electron-exchange matrix element is

$$T_{DA} = \sum_{i=1}^{N} V_{DA}^{(i)} \qquad (11)$$

subject to the perturbation condition that $V_{D(B1)}^{(1)}$, $V_{(B1)(B2)}^{(1)}$, ..., $V_{(BN)A}^{(1)} < E_D - E_{BJ}'$....

Equations 5–11 have the following implications for practical use of superexchange theory:

(a) Equations 8–11 can be combined with eqs 5 and 6 in a Condon scheme where the electronic and nuclear factors are separated, provided that the intermediate states are "high-energy" states. This means that their potential surfaces at the crossing region between the reactant and product surfaces are located well above this region (Figure 1a). If the intermediate states have low energies as in Figure 1b, then the system is temporarily physically located in the vibrationally intermediate states and undertakes an entangled trajectory on the potential surfaces before proceeding to the acceptor state. This endows the superexchange mechanism with a quite different character, such as shown in detail elsewhere.[22c,25,70,77]

(b) The energy denominators in eqs 9 and 10 include the vibrational energy differences in the nonequilibrium nuclear configurations at the moment of electron transfer (Figure 1a); i.e. the energy denominators are taken at the configuration Q*. Since Q* depends on the reaction free energy, so must the superexchange matrix element. The dependence is approximately quadratic for the second-order terms, which represents a single intermediate state, but stronger for higher order terms, which represent superexchange through a large number of intermediate states.

(c) If all intermediate state exchange matrix elements and energy denominators coincide and take the values β and Δ, respectively, the simple form first derived by McConnell[74] is obtained

$$V_{DA}^{(N)} = \frac{\beta_D \beta_A}{\Delta}(\beta/\Delta)^{N-1} \qquad (12)$$

for the Nth-order term, where β_D and β_A are short-hand notations for $V_{D(B1)}^{(1)}$ and $V_{(BN)A}^{(1)}$, respectively. Equation 12 can be recast in the exponential form[67]

$$V_{DA}^{(N)} = \frac{\beta_D \beta_A}{\beta} \exp\left[-\left(\frac{1}{a} \ln \frac{\Delta}{\beta}\right) R\right] \qquad (13)$$

where a is the average geometric extension of the intermediate groups along the ET path. The condition that all energy gaps coincide is, however, an unlikely event when the intermediate electronic states are strongly coupled to local or environmental nuclear modes, even when the equilibrium free energies coincide, but in this sense superexchange ET through excited, weakly localized protein electronic states can perhaps be regarded as weakly coupled to environmental nuclear modes.

(d) Equations 9–12 show that suitable aromatic amino acid fragments in an aliphatic chain might increase the rate constant due to more favorable energy denominators. In tunnel theory this corresponds to an "indentation" or "hole" in the barrier, in the limit of a deep hole converting the tunnel process to a resonance tunnel event.[70,71] The barrier fluctuation effect is, however, not likely to exceed 1 or 2 orders of magnitude.[63,70] Larger effects arise if the intermediate group energy is close to the donor or the acceptor level so that superexchange proceeds through a vibrationally unrelaxed real intermediate state.[77,78] In this case the intermediate-state energy is also reflected in the activation factor.[22c,25,70,77,78] This could be a reason for a rate enhancement by 4 orders of magnitude on Tyr or Phe substitution of Ser or Gly in ET between oxidized Zn-substituted cytochrome peroxidase and cyt c(II), where the unstable Zn porphyrin radical energy is close to that of inserted intermediate Tyr or Phe.[79]

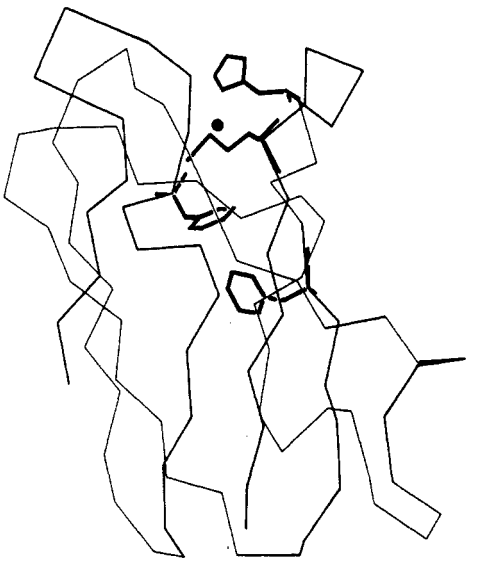

Figure 2. Poplar PC(II) structure, applying also to PC(I), at pH = 7.5. Coordinated His-87 and the Met-92/Phe-14/Phe-82 ET channel are indicated by bold lines. The almost perpendicular orientation of the two phenyl rings is noted. Coordinates are from ref 81 and the Brookhaven Data bank.[82] Evans and Sutherland PS 300 computer graphics were used.

In the next section we provide an extended Hückel estimate of the electron-exchange matrix element for ET at the two binding sites which suggests that two ET pathways could in fact be electronically competitive. This conclusion also emerges from the following simple consideration. Orbital decay factors of the exchange matrix elements for ET between transition-metal complexes containing aqua or aromatic organic ligands[50,51] are in the range 1.2–2 Å^{-1}. Similar values are obtained from eq 13 for superexchange ET assisted by water for $\beta \approx \beta_D \approx \beta_A \approx 0.1$ eV and $\Delta \approx 5$–10 eV. Δ/β for ET through protein is much smaller. Values obtained for intramolecular ET through aliphatic and aromatic bridges in synthetic complexes are in this respect suitable limits. These values are 10–20 and 4, respectively,[67] giving for the orbital exponent of the superexchange matrix element $\alpha_{sup\ ex} = 0.3$–0.6 Å^{-1}.

The orbital exponent for ET through the organic material is thus clearly smaller than for direct or water-assisted ET, due to the weaker nearest-neighbor overlap and larger energy gap for the former, and superexchange, dominates as R increases. In the frequently used form $V_{DA}^{(1)} = V_{DA}^{\circ(1)} \exp(-\alpha_{dir} R)$, $V_{DA}^{\circ(1)} \approx 10$ eV,[67] this happens at $R \approx 5$–7 Å when $\alpha_{sup\ ex} \approx 0.3$ Å^{-1} and at $R \approx 7$–10 Å for $\alpha_{sup\ ex} \approx 0.6$ Å^{-1}. These values are compatible with the two surface-site distances from the copper atom in plastocyanin, and it is understandable that the longer distance ET route through protein could compete with shorter distance ET at the adjacent binding site.

4. Extended Hückel Calculation of Direct and Superexchange ET Pathways at Adjacent and Remote Binding Sites of Plastocyanin

In this section we consider a quantum approach to the electronic factor for ET at the adjacent binding site and for ET along several geometrically suitably located pathways leading from the remote binding site to the copper atom through the protein. The basis

(77) (a) Vol'kenshtein, M. V.; Dogonadze, R. R.; Madumarov, A. K.; Kharkats, Yu. I. *Dokl. Akad. Nauk SSSR, Ser. Fiz. Khim.* **1971**, *199*, 124. (b) Dogonadze, R. R.; Kharkats, Yu. I.; Ulstrup, J. *J. Electroanal. Chem. Interfacial Electrochem.* **1972**, *39*, 47. (c) Kharkats, Yu. I.; Madumarov, A. K.; Vorotyntsev, M. A. *J. Chem. Soc., Faraday Trans. 2* **1974**, *70*, 1578. (d) Kuznetsov, A. M.; Kharkats, Yu. I. *Elektrokhimiya* **1976**, *12*, 1277. (e) Kuznetsov, A. M.; Ulstrup, J. *J. Chem. Phys.* **1981**, *75*, 2047.

(78) (a) Mukamel, S.; Yan, Y. J. *Acc. Chem. Res.* **1989**, *22*, 301. (b) Hu, Y.; Mukamel, S. *Chem. Phys. Lett.* **1989**, *160*, 140.

(79) Liang, N.; Pielak, G. J.; Mauk, A. G.; Smith, M.; Hoffman, B. M. *Proc. Nat. Acad. Sci. U.S.A.* **1987**, *84*, 1249.

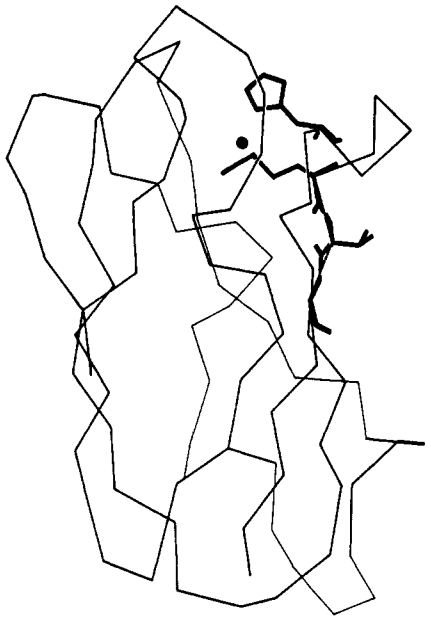

Figure 3. Poplar PC(II) structure. His-87 and the Met-92/Val-93/Gly-94 channel are indicated by bold lines. Coordinates and graphics are as in Figure 2.

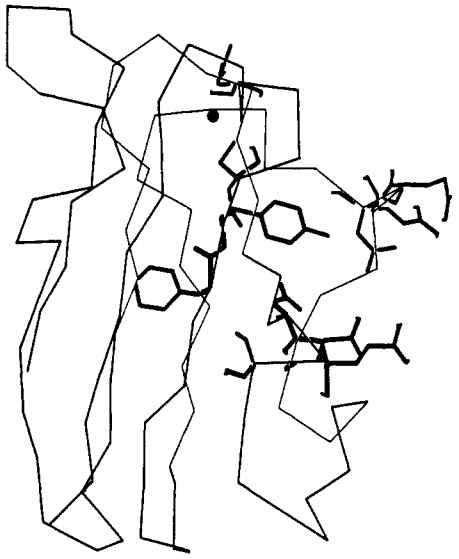

Figure 4. Poplar PC(II) structure. His-87 (sideways, top) and the ET sequence Cys-84/Tyr-83/Phe-82 are indicated by bold lines. The protrusion of the Tyr-83 phenol group is noted. The negatively charged 42–45 (bottom) and 59–61 (top) groupings on either side of Tyr-83 are also indicated by bold lines.

for the choice of protein ET pathways was an Evans and Sutherland PS 300 graphic display of the three-dimensional poplar PC(II) structure reported by Freeman and his associates.[80] The choice of PC(II) avoids "unusual" geometries caused by possible dissociation of the His-87 ligand and is an adequate reproduction of PC(I) at neutral pH.[16-19]

The three-dimensional structure suggests that four pathways of appropriately aligned amino acid fragments shown in Figures 2–4 constitute suitable ET channels between the copper center and the remote binding site. These are (1) Cu/Me-92/Phe-14/Phe-82/D, (2) Cu/Met-92/Val-93/Gly-94/D, (3) Cu/Cys-84/Tyr-83/D, and (4) Cu/Cys-84/Tyr-83/Phe-82/D.

In addition, the adjacent site ET path is (5) Cu/His-87/D. "D" stands for a suitable donor molecule noncovalently associated with the binding sites. In the present calculations this molecule is chosen as a protonated pyridine anion radical with an N–H bond length of 1.04 Å. The detailed electronic structure of the pyridine anion radical is available from previous investigations.[81]

(80) Guss, J. M.; Freeman, H. C. *J. Mol. Biol.* **1983**, *169*, 521.

Table I. Overall Electron-Exchange Matrix Elements for the Four Superexchange ET Channels from the Remote Binding Site and for "Direct" ET at the Adjacent Binding Site

channel no.	1	2	3	4	5
T_{DA}, cm^{-1}	1.1×10^{-9}	3×10^{-4}	6×10^{-2}	6×10^{-4}	0.4

The following additional general points are important in relation to the choice of ET pathways and electronic structure calculations:

(a) The calculations incorporate the four copper ligands His-37, Cys-84, His-87, and Met-92 in addition to the ET amino acid channels and the protonated pyridine anion radical.

(b) The hydrogen atoms and amino acid bond reconstitution have been added to the crystal structure by the program HGEN, developed by S. E. V. Phillips, Department of Biophysics, The University of Leeds, Leeds, U.K.

(c) Channels 2 and 3 represent covalent through-bond ET pathways leading from geometrically accessible surface sites in the region of the negatively charged remote binding site to the copper atom. Channel 4 contains an additional covalent Phe-82 link, while channel 1 contains both Phe-82 and two through-space links. Phe-82 is not directly accessible to the surface. Its incorporation is prompted by its location close to the group of negatively charged 42–45 residues, which is a likely site of ET probe attachment in Cr(III)-attachment experiments.[8,33]

(d) The ET channels contain both aliphatic and aromatic residues.

The electron-exchange matrix elements and energy gaps in section 3 (cf. the Appendix) were calculated by the extended Hückel method.[83-85] This approach is rather crude and gives poor values in absolute terms but is a useful and tractable method for large molecular systems and a fairly reliable frame for qualitative trends and semiquantitative comparisons such as relating to the relative efficiency of the different ET channels listed above.

The calculations provide the LCAO MO's and the associated energies for the molecular systems that constitute the five ET channels. The quantities are recast in the form of MO's and energies of individual molecular fragments (the copper atom with ligands, amino acids, and molecular donor) and exchange-coupling matrix elements between the fragments, H_{ij}. The latter are obtained from the overlap integrals, S_{ij}, by a modified form of the Wolfsberg–Helmholtz relation for adjacent atom coupling[85]

$$H_{ij} = \tfrac{1}{2}\chi_{ij}(H_{ii} + H_{jj})S_{ij} \qquad (14)$$

H_{ii} and H_{jj} are normally the single-electron energy eigenvalues for the atomic orbitals i and j, respectively, and χ_{ij} is an empirically determined parameter. We have applied the procedure of Pietro, Marks, and Ratner[86] and substituted the single-electron energies H_{ii} and H_{jj} by the MO energies of interacting fragments and S_{ij} by the corresponding molecular fragment overlap integrals. In addition, in view of the similarity between the systems investigated in ref 86 and the ET channels in PC, we have used the value of $\chi_{ij} = 0.50$ from ref 84 rather than 1.75 for interatomic coupling. This low value ensures the most restrictive evaluation.

The extended Hückel MO energies and exchange-coupling factors can be directly inserted in the ET transition matrix ele-

(81) Mikkelsen, K. V.; Ratner, M. A. *J. Chem. Phys.* **1989**, *90*, 4237.
(82) (a) Bernstein, F. C.; Koetzle, T. F.; Williams, G. J. B.; Meyer, E. F., Jr.; Brice, M. D.; Rodgers, J. R.; Kennard, O.; Shimanouchi, T.; Tasumi, M. *J. Mol. Biol.* **1977**, *112*, 535. (b) Abola, E. E.; Bernstein, F. C.; Bryant, S. H.; Koetzle, T. F.; Weng, J. In *Crystallographic Databases—Information Content, Software Systems, Scientific Applications*; Allen, F. H., Bergerhoff, G., Sievers, R., Eds.; Data Commission of the International Union of Crystallography: Born/Cambridge/Chester, 1987; p 107.
(83) (a) Hoffman, R. *J. Chem. Phys.* **1962**, *37*, 2872. (b) Hoffman, R. *J. Chem. Phys.* **1963**, *39*, 1397.
(84) Ammeter, J. H.; Bürgi, H.-B.; Thibeault, J. C.; Hoffmann, R. *J. Am. Chem. Soc.* **1978**, *100*, 3686.
(85) Wolfsberg, M.; Helmholtz, L. *J. Chem. Phys.* **1952**, *20*, 837.
(86) Pietro, W. J.; Marks, T. J.; Ratner, M. A. *J. Am. Chem. Soc.* **1985**, *107*, 5387.

Table II. Exchange Matrix Elements, V (eV), and Energy Gaps, ΔE (eV), for ET along Different PC Channels[a]

Channel No. 1

	Pyr-H/ Phe-82	Phe-82/ Phe-14	Phe-14/ Met-92	Met-92/ Cu
V	1×10^{-2}	4×10^{-5}	1×10^{-5}	5×10^{-3}
$\lvert\Delta E\rvert$	0.32	0.27	1.71	

Channel No. 2

	Pyr-H/ Gly-94	Gly-94/ Val-93	Val-93/ Met-92	Met-92
V	1×10^{-2}	3×10^{-2}	4×10^{-2}	5×10^{-3}
$\lvert\Delta E\rvert$	1.60	0.56	1.71	

Channel No. 3

	Pyr-H/ Tyr-83	Tyr-83/ Cys-84	Cys-84/ Cu
V	1×10^{-2}	3×10^{-2}	2×10^{-2}
$\lvert\Delta E\rvert$	0.59	1.31	

Channel No. 4

	Pyr-H/ Phe-82	Phe-82/ Tyr-83	Tyr-83/ Cys-84	Cys-84/ Cu
V	1×10^{-2}	3×10^{-3}	3×10^{-2}	2×10^{-2}
$\lvert\Delta E\rvert$	0.32	0.59	1.31	

Channel No. 5

	Pyr-H/His-87	His-87/Cu
V	1.6×10^{-2}	9×10^{-3}
$\lvert\Delta E\rvert$	2.73	

[a] ΔE refers to the energy difference between the protonated pyridine anion radical, pyr-H, and the amino acid fragment at the consecutive places in the channel sequences toward the Cu atom.

ments for the five ET channels and supplemented by the overlap integral between the donor and the first group orbital. This overlap value was always chosen as 3.0×10^{-3}, which is appropriate for two suitably spaced small aromatic molecules.[50,51] The resulting overall exchange matrix elements thus basically reflect the electronic properties of the different protein ET channels.

Table I shows the resulting overall exchange matrix elements for the five ET channels. Figures 2–4 reveal three features in particular:

(a) The different protein channels are highly selective, giving a span of 6 or 7 orders of magnitude in T_{DA}.

(b) The through-bond paths (channels 2–4) are much more efficient than the through-space path (channel 1).

(c) The electron-exchange matrix element is higher for the path at the adjacent binding site than for all the remote binding sites. However, one of the remote binding site channels (channel 3) is almost as efficient as the adjacent-site path. This channel seems to be the only channel competitive with adjacent-site ET and involves Tyr-83 as the intermediate residue in direct contact with the electron donor at the protein surface. Data from protein modification[21] and NMR[26-29] studies have in fact pointed to the importance of this group in ET and ionic association.

Table II shows more detail about the channel efficiencies. The following should be noted:

(d) The electron-exchange matrix elements between the individual fragments are always smaller than the energy gaps, suggesting that the superexchange view is appropriate.

(e) The very small value of T_{DA} for channel 1 is mainly caused by the poor overlap between Phe-14 and both Phe-82 and Met-92. These overlaps represent through-space interactions, and the two aromatic rings are furthermore almost perpendicular to each other, giving an unfavorable overlap symmetry.

(f) The electron-exchange matrix elements for the aliphatic chain in channel 2 are more favorable than the matrix elements in channel 1 by about 3 orders of magnitude. This emphasizes the importance of through-bond interaction.

(g) Channels 2 and 4 are almost equally efficient, more favorable energy denominators in the largely aromatic channel 4 being compensated by more favorable electron-exchange matrix elements in the aliphatic channel 2.

(h) When channel 4 is shortened by the Phe-82 link, a very favorable ET path involving only Tyr-83 between the Cys-84 ligand and the protein surface remains. This seems to be the only channel that can compete effectively with ET at the adjacent binding site.

(i) ET at the adjacent binding site has the largest overall transition matrix element of all the ET paths considered. However, in spite of the much shorter ET distance, it is only a factor of 7 larger than for the most favorable remote-site ET route. The relatively inefficient adjacent-site ET mechanism is caused both by a relatively unfavorable Cu/His-87 overlap and by a large energy gap between pyr-H and His-87.

(j) The average decrease in electronic coupling per amino acid residue is 155, 40, and 60 for the through-bond channels, 2–4, respectively, and about 10^4 per residue for through-space links. For average geometric amino acid extensions of 5–7 Å this corresponds to α values (cf. eq 4) of 1.4–2, 1–1.4, and 1.2–1.6 $Å^{-1}$ for the three through-bond channels and 2.6–3.6 $Å^{-1}$ for the through-space links. The decrease per link fluctuates, however, considerably in each through-bond channel and varies from 15–400, 20–60, and 20–100, corresponding to "local" decay factors in the ranges 0.8–2.4, 0.8–1.6, and 0.8–1.8 $Å^{-1}$ for channels 2–4, respectively. The values are higher than the estimates in section 3 due to the low values of the exchange matrix elements, but the relative, rather than the absolute, values are of primary importance here. It should then be noted that there is some variation in the average decay features of the channels and that the decay parameter is smallest for channel 3. The substantial fluctuations in individual links imply, however, that the concept of approximately constant decay per amino acid in a polypeptide chain should be applied with care (cf. ref 87).

We finally notice that similar calculations for direct through-space ET from pyr-H at positions close to the remote binding site to the ligated copper atom, disregarding the rest of the protein altogether, give entirely vanishing electron-exchange matrix elements.

5. Concluding Remarks

The superexchange formalism suggests that intramolecular through-bond ET in metalloproteins not only can be brought to occur but also can be electronically competitive with direct outer-sphere ET over significantly shorter distances where the electronic wave functions are not modulated by "matter" or modulated by the solvent only. This is due to the much slower electronic density decay through the protein, associated with more favorable through-bond overlaps and energy gaps.

We have substantiated this by extended Hückel calculations for five selected ET pathways leading from the remote and adjacent binding sites in plastocyanin to the copper atom, as suggested by the crystallographic structure of plastocyanin. While fraught with the general reservations as to the reliability of this approach, the results still suggest that potential ET channels are highly selective and depend crucially on the overlaps, relative orientations, and LUMO energies of the intermediate-group fragments. Through-bond pathways appear to be much more efficient than through-space pathways, suggesting that long-range ET in metalloproteins and other structurally anisotropic materials should be supplemented by more detailed views than geometric distance relations.

The calculations show specifically that the electronic transmission coefficient for the Cu/Cys-84/Tyr-83 remote binding site pathway is close to being electronically competitive with ET at the adjacent binding site. Since the remote site is associated with favorable work terms for positively charged reaction partners, it is therefore understandable that this path can dominate the overall kinetics for this group of reaction partners, such as suggested by many experimental observations.

(87) Beratan, D. N.; Onuchic, J. N.; Hopfield, J. J. *J. Chem. Phys.* **1987**, *86*, 4488.

Acknowledgment. We wish to thank the Danish Natural Science Research Council, Otto Mønsteds Fond, Direktør Ib Henriksens Fond, Lundbeckfonden, and Brødrene Hartmann's Fond for financial support. We also thank Dr. Jens Nyborg, The University of Aarhus, for great help with the computer graphics and Dr. M. D. Newton, Brookhaven National Laboratory, for details on electronic structure calculations prior to publication.

Appendix

Derivation of the Exchange Matrix Elements. We derive here the general superexchange perturbation terms by means of time-evolution operators and the time-dependent Schrödinger equation. The system consists of the donor molecule, the number of spin orbitals and electrons of which are S_D and N_D, respectively, the assembly of bridge groups numbered $J = 1, ..., N$ with S_J spin orbitals and N_J electrons, and the acceptor molecule with N_A electrons and S_A spin orbitals. The MO basis set is derived from all the donor, acceptor, and bridge group orbitals by using symmetric orthogonalization. The electron number operators for the donor, acceptor, and bridge groups are, in second quantization[88]

$$\hat{N}_D = \sum_{S\in D} a_S^+ a_S \qquad \hat{N}_A = \sum_{S\in A} a_S^+ a_S$$
$$\hat{N}_{BJ} = \sum_{S\in BJ} a_S^+ a_S \quad (J = 1, ..., N) \tag{A.1}$$

a_S^+ and a_S being the appropriate creation and annihilation operators, respectively.

The total number operator is

$$\hat{N}_T = \hat{N}_D + \hat{N}_A + \sum_{J=1}^{N} \hat{N}_{BJ} \tag{A.2}$$

The initial, final, and intermediate states are eigenstates of the number operators $\hat{N}_D$, $\hat{N}_A$, and $\hat{N}_{BJ}$ ($J = 1, ..., N$). The initial- and final-state wave functions are

$$\Phi_D = |1, ..., N_D, N_D + 1; 1, ..., N_{B1}; 1, ..., N_{B2}; ...; 1, ..., N_{BN}; 1, ..., N_A\rangle$$
$$\Phi_A = 1, ..., N_D; 1, ..., N_{B1}; 1, ..., N_{B2}; ...; 1, ..., N_{BN}; 1, ..., N_A, N_A + 1\rangle \tag{A.3}$$

The intermediate state corresponding to electron localization on the Jth bridge group is

$$\Phi_{BJ} = |1, ..., N_D; 1, ..., N_{B1}; 1, ..., N_{B2}; ...; 1, ..., N_{BJ}, N_{BJ} + 1; ...; 1, ..., N_{BN}; 1, ..., N_A\rangle \tag{A.4}$$

The corresponding state for hole transfer is

$$\Phi_{BJ}^h = |1, ..., N_D, N_D + 1; 1, ..., N_{B1}; 1, ..., N_{B2}; ...; 1, ..., N_{BJ} - 1; ...; 1, ..., N_{BN}; 1, ..., N_A, N_A + 1\rangle \tag{A.5}$$

Electron and hole transfer can be treated quite similar ways, but we consider explicitly only electron transfer.

The wave functions thus satisfy the equations

$$\hat{N}_D\Phi_D = (N_D + 1)\Phi_D \qquad \hat{N}_A\Phi_D = N_A\Phi_D \qquad \hat{N}_{BJ}\Phi_D = N_{BJ}\Phi_D$$
$$\hat{N}_D\Phi_{BJ} = N_D\Phi_{BJ} \qquad \hat{N}_A\Phi_{BJ} = N_A\Phi_{BJ}$$
$$\hat{N}_{BJ}\Phi_{BJ} = (N_{BJ} + 1)\Phi_{BJ}$$
$$\hat{N}_D\Phi_A = N_D\Phi_A \qquad \hat{N}_A\Phi_A = (N_A + 1)\Phi_A$$
$$\hat{N}_{BJ}\Phi_A = N_{BJ}\Phi_A \tag{A.5a}$$

The total system Hamiltonian is divided into a zero-order Hamiltonian, $\hat{H}_0$, and a perturbation, $\hat{V}$, which couples the different molecular entities, i.e.

$$\hat{H} = \hat{H}_0 + \hat{V} \tag{A.6}$$

We restrict ourselves to the limit where the zero-order Hamiltonian and the perturbation coincide for all the electronic states. Generalization to incorporate nonorthogonality can be effected by scattering matrix theory, cf. ref 75 and discussions in refs 22–25. The functions Φ_D, Φ_A, and all the Φ_{BJ}'s are then regarded as eigenfunctions of $\hat{H}_0$, i.e.

$$\hat{H}_0\Phi_D = E_D\Phi_D \qquad \hat{H}_0\Phi_A = E_A\Phi_A \qquad \hat{H}_0\Phi_{BJ} = E_{BJ}\Phi_{BJ} \tag{A.7}$$

where E_D, E_A, and E_{BJ} are the eigenvalues.

We now solve the time-dependent Schrödinger equation

$$i\hbar\frac{\delta\psi(t)}{\delta t} = (\hat{H}_0 + \hat{V})\psi(t) \tag{A.8}$$

subject to the condition that

$$\psi(t = -\infty) = \Phi_D \tag{A.9}$$

since the "excess" electron density is located on the donor prior to reaction. The solution is the reaction matrix for finding the excess electron on the acceptor at $t = 0$.

In the interaction representation, wave functions and operators, A, take the form

$$\psi_I(t) = e^{iH_0t/\hbar}\psi(t) \qquad A_I(t) = e^{iH_0t/\hbar}Ae^{-iH_0t/\hbar} \tag{A.10}$$

Moreover, the expectation value of A is independent of the representation, i.e.

$$\langle A\rangle = \langle\psi(t)|A|\psi(t)\rangle = \langle\psi_I(t)|e^{iH_0t/\hbar}|A|e^{-iH_0t/\hbar}\psi_I(t)\rangle = \langle\psi_I(t)|A_I(t)|\psi_I(t)\rangle \tag{A.11}$$

The time-dependent Schrödinger equation is, in the interaction representation

$$i\hbar\frac{\delta\psi_I(t)}{\delta t} = V_I(t)\psi_I(t) \tag{A.12}$$

The solution is, in integral form

$$\psi_I(t) = \psi_I(t_0) - \frac{i}{\hbar}\int_{t_0}^{t} dt_1 V_I(t_1)\psi_I(t_1) \tag{A.13}$$

where the limits $t \to 0$ and $t_0 \to \infty$ have to be inserted. By addition of the factor $\exp(-\epsilon|t|/\hbar)$, $\epsilon \to 0+$, to ensure convergency, integration gives

$$\psi_I(t = 0) \equiv \psi_R = \Phi_D - \frac{i}{\hbar}\lim_{\epsilon\to 0+}\int_{-\infty}^{0} dt_1\, e^{-\epsilon|t_1|/\hbar}V_I(t_1)\psi_I(t_1) \tag{A.14}$$

The iterative solutions take the form

$$\psi_R = \Phi_D + \lim\frac{1}{E_D - H_0 + i\epsilon}V\psi_R =$$
$$\Phi_D + \lim_{\epsilon\to 0+}\frac{1}{E_D - H_0 + i\epsilon}V\Phi_D +$$
$$\lim_{\epsilon\to 0+}\frac{1}{E_D - H_0 + i\epsilon}V\frac{1}{E_D - H_0 + i\epsilon}V\Phi_D + ... \tag{A.15}$$

The overall transition matrix element (scattering amplitude) is

$$T_{DA} = \langle\Phi_A|V|\Psi_R\rangle =$$
$$\langle\Phi_A|V|\Phi_D\rangle + \lim_{\epsilon\to 0+}\sum_{B,\alpha}\frac{\langle\Phi_A|V|\Phi_{B\alpha}\rangle\langle\Phi_{B\alpha}|V|\Psi_R\rangle}{E_D - E_{B\alpha} + i\epsilon} \tag{A.16}$$

where B represents all conceivable intermediate groups and α all electronic states of these groups. Continuing the iteration, we obtain

$$T_{DA} = \langle\Phi_A|V|\Phi_D\rangle + \lim_{\epsilon\to 0+}\sum_{B,\alpha}\frac{\langle\Phi_A|V|\Phi_{B\alpha}\rangle\langle\Phi_{B\alpha}|V|\Phi_D\rangle}{E_D - E_{B\alpha} + i\epsilon} + ... +$$
$$\lim_{\epsilon\to 0+}\sum_{B,\alpha}^{(1)}\sum_{B,\beta}^{(2)}...\sum_{\xi}^{(N)}\frac{\langle\Phi_A|V|\Phi_{B\alpha}\rangle\langle\Phi_{B\alpha}|V|\Phi_{B\beta}\rangle...\langle\Phi_B|V|\Phi_A\rangle}{(E_D - E_{B\alpha})(E_D - E_{B\beta})...(E_D - E_{B\xi})} \tag{A.17}$$

Greek letters again representing different electronic states in the various intermediate bridge groups. The first term in eq A.17 represents direct coupling between D and A. The second term accounts for coupling between D and A via any of the intermediate groups—where the index "J" has been omitted—and via all

(88) See for example: Linderberg, J.; Öhrn, Y. *Propagators in Quantum Chemistry*; Academic Press: New York, 1973.

possible electronic states in these groups. Subsequent terms represent analogous ET percolation routes through all combinations of bridge groups and their different electronic states.

If only nearest-neighbor interactions are important, eq A.17 is drastically simplified. Only a single group of terms remains, namely the Nth order term

$$T_{DA} = \sum_{\alpha}\sum_{\beta}\cdots\sum_{\xi}\frac{V_{D,(B1)}^{(1)}V_{(B1)\beta,(B2)\gamma}^{(1)}\cdots V_{(BN)\xi,A}^{(1)}}{(E_D - E_{(B1)\beta})(E_D - E_{(B2)\gamma})\cdots(E_D - E_{(BN)\xi})} \quad (A.18)$$

where $V_{D(B1)\beta}^{(1)} \equiv \langle\Phi_D|V|\Phi_{(B1)\beta}\rangle$, etc. In principle eq A.18 incorporates all conceivable combinations of superexchange and hole transfer mechanisms. If furthermore only a single electronic state on each bridge group contributes, then T_{DA} is further reduced, giving

$$T_{DA} = V_{DA}^{(N)} = \frac{V_{D(B1)}^{(1)}V_{(B1)(B2)}^{(1)}\cdots V_{(BN)A}^{(1)}}{(E_D - E_{B1})(E_D - E_{B2})\cdots(E_D - E_{BN})} \quad (A.19)$$

which is the form used in eq 8 and in the extended Hückel calculations.

Contribution from the Department of Organic Chemistry, University of Groningen, Nijenborgh 16, 9747 AG Groningen, The Netherlands

Bimetallic Oxidation Catalysts. Synthesis, X-ray Analysis, and Reactivity of a Binuclear *p*-Hydroquinone-Containing Copper(II) Complex

Onko Jan Gelling, Auke Meetsma, and Ben L. Feringa*

Received August 3, 1989

The new pentadentate ligand 1,3-bis[*N*-2-(2'-pyridylethyl)formimidoyl]-2,5-dihydroxybenzene (**1**) was prepared in five steps from 2,6-dimethylphenol in 21% overall yield. Reaction of **1** with $Cu^{II}(ClO_4)_2{\cdot}6H_2O$ gave the unexpectedly stable hydroquinone-containing binuclear Cu(II) complex [2,6-bis[*N*-2-(2'-pyridylethyl)formimidoyl]-4-hydroxy-1-phenolato]biscopper(II) bisperchlorate (**8**). The crystal and molecular structure of **8** was determined by X-ray analysis. The complex crystallizes in the triclinic space group $P\bar{1}$, with $Z = 2$ in a unit cell of the following dimensions: $a = 9.399$ (2) Å, $b = 10.469$ (1) Å, $c = 14.612$ (4) Å, $\alpha = 102.72$ (2)°, $\beta = 100.71$ (2)°, $\gamma = 104.60$ (2)°. Surprisingly high reactivity of **8** was observed in catalytic oxidations of hydroquinones and α-hydroxy ketones using molecular oxygen as the oxidant. A mechanistic discussion is provided.

Currently much effort is devoted to develop useful catalytic systems for mild and selective oxidations with the aid of molecular oxygen.[1] Furthermore it is of great interest to elucidate the factors that determine the (reversible) binding and activation of O_2 in various natural oxygen transport systems and mono- and dioxygenases and to mimic their activity.[2] Guided by nature, intriguing model systems[3] for copper-containing enzymes such as hemocyanin[2,4] have been developed. Considerable progress has been made in order to establish the active species in cytochrome P450 and related oxygenases.[5] Contrary to the successful development of oxidation catalysts based on metalloporphyrins,[6] synthetically useful catalysts based on copper complexes that act as mimics for copper-containing monooxygenases (e.g. tyrosinase

Scheme I

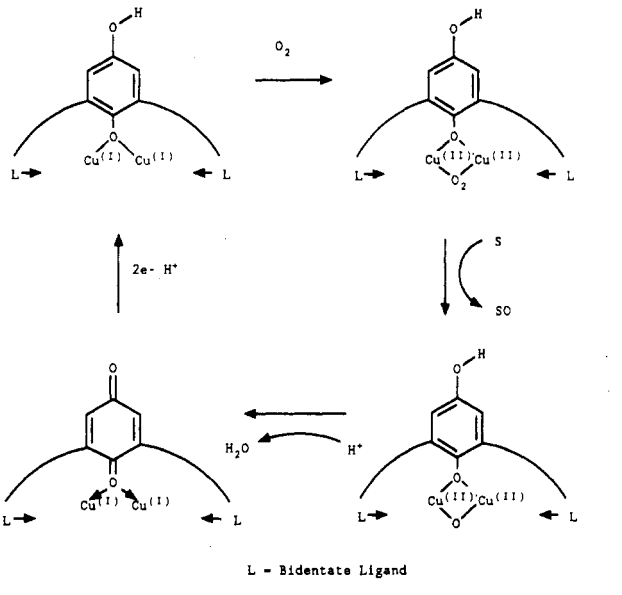

(1) Sheldon, R. A.; Kochi, J. K. *Metal-Catalyzed Oxidations of Organic Compounds*; Academic Press: New York, 1981. *Oxygen Complexes and Oxygen Activation by Transition Metals*; Martell, A. E., Sawyer, D. T., Eds.; Plenum: New York, 1988.

(2) *Copper Proteins and Copper Enzymes*; Lontie, R., Ed.; CRC: Boca Raton, FL, 1984; Vol. 2. *Copper Coordination Chemistry: Biochemical & Inorganic Perspectives*; Karlin, K. D., Zubieta, J., Eds.; Adenine: Guilderland, NY, 1983. *Copper Proteins*; Sigel, H., Ed.; Metal Ions in Biological Systems, Vol. 13; Marcel Dekker: New York, 1981. Niederhoffer, E. C.; Timmons, J. H.; Martell, A. E. *Chem. Rev.* **1984**, *84*, *137*. Solomon, E. I. In *Metal Ions in Biology*; Spiro, T. G., Ed.; Wiley-Interscience: New York, 1981; Vol. 3, p 44.

(3) (a) Karlin, K. D.; Gultneh, Y.; Hutchinson, J. P.; Zubieta, J. *J. Am. Chem. Soc.* **1982**, *104*, 5240. (b) Pate, J. E.; Cruse, R. W.; Karlin, K. D.; Solomon, E. I. *J. Am. Chem. Soc.* **1987**, *109*, 2624. (c) Traylor, T. G.; Hill, K. W.; Tian, Z. Q.; Rheingold, A. L.; Peisach, J.; McCracken, J. *J. Am. Chem. Soc.* **1988**, *110*, 5571. (d) Nelson, S. M. *Inorg. Chim. Acta* **1982**, *62*, 39. (e) Sorrell, T. N.; Malachowski, M. R.; Jameson, D. L. *Inorg. Chem.* **1982**, *21*, 3250. (f) Bulkowski, J. E.; Burk, P. L.; Ludmann, M. F.; Osborn, J. A. *J. Chem. Soc., Chem. Commun.* **1977**, 498. (g) Simmons, M. G.; Merrill, C. L.; Wilson, L. J.; Bottomley, L. A.; Kadish, K. M. *J. Chem. Soc., Dalton Trans.* **1980**, 1827. (h) Karlin, K. D.; Cruse, R. W.; Gultneh, Y.; Hayes, J. C.; Zubieta, J. *J. Am. Chem. Soc.* **1984**, *106*, 3372. (i) Pate, J. E.; Cruse, R. W.; Karlin, K. D.; Solomon, E. I. *J. Am. Chem. Soc.* **1987**, *109*, 2624. (j) McKee, V.; Zvagulis, M.; Dagdigian, J. V.; Patch, M. G.; Reed, C. A. *J. Am. Chem. Soc.* **1984**, *106*, 4765. (k) Karlin, K. D.; Haka, M. S.; Cruse, R. W.; Meyer, G. J.; Faroog, A.; Gultneh, Y.; Hayes, J. C.; Zubieta, J. *J. Am. Chem. Soc.* **1988**, *110*, 1196. (l) Jacobson, R. R.; Tyeklar, Z.; Faroog, A.; Karlin, K. D.; Liu, S.; Zubieta, J. *J. Am. Chem. Soc.* **1988**, *110*, 3690. (m) Cruse, R. W.; Kaderli, S.; Karlin, K. D.; Zuberbühler, A. D. *J. Am. Chem. Soc.* **1988**, *110*, 6882.

(4) Solomon, E. I.; Penfield, K. W.; Wilcox, D. E. *Struct. Bonding (Berlin)* **1983**, *53*, 1. Karlin, K. D.; Gultneh, Y. *J. Chem. Educ.* **1985**, *62*, 893. Gaykema, W. P. J.; Hol, W. G. J.; Verreyken, J. M.; Soeter, N. M.; Bak, H. J.; Beintema, J. J. *Nature (London)* **1984**, *309*, 23. Linzen, B.; Soeter, N. M.; Riggs, A. F.; Schneider, H. J.; Schartau, W.; Moore, M. D.; Yokota, E.; Behrens, P. Q.; Nakashima, H.; Takagi, T.; Nemoto, T.; Verreyken, J. M.; Bak, H. J.; Beintema, J. J.; Volbeda, A.; Gaykema, W. P. J.; Hol, W. G. J. *Science (Washington, D.C.)* **1985**, *229*, 519.

(5) *Cytochrome P-450, Structure, Mechanism and Biochemistry*; Ortiz de Montellano, P. R., Ed.; Plenum Press: New York, 1986.

(6) Groves, J. T.; Nemo, T. E.; Meyers, R. S. *J. Am. Chem. Soc.* **1979**, *101*, 1032. Chang, C. K.; Kuo, M.-S. *J. Am. Chem. Soc.* **1979**, *101*, 3413. Gelb, M. H.; Toscano, W. A., Jr.; Sligar, S. G. *Proc. Natl. Acad. Sci. U.S.A.* **1982**, *79*, 5758. Guilmet, E.; Meunier, B. *Nouv. J. Chim.* **1982**, *6*, 511. Traylor, T. G.; Marsters, J. C., Jr.; Nakano, T.; Dunlap, B. E. *J. Am. Chem. Soc.* **1985**, *107*, 5537. Collman, J. P.; Brauman, J. I.; Meunier, B.; Hayashi, T.; Kodadek, T. *J. Am. Chem. Soc.* **1985**, *107*, 2000. Tabushi, I. *Coord. Chem. Rev.* **1988**, *86*, 1. Groves, J. T.; Meyers, T. S. *J. Am. Chem. Soc.* **1983**, *105*, 5791 and references cited therein.

0020-1669/90/1329-2816$02.50/0